Composites Science and Technology 69 (2009) 139–146

Contents lists available at ScienceDirect

Composites Science and Technology

journal homepage: www.elsevier.com/locate/compscitech

Influence of additives on the global mechanical behavior and the microscopic strain localization in wood reinforced polypropylene composites during tensile deformation investigated using digital image correlation

A. Godara [a,b,*], D. Raabe [c], I. Bergmann [d], R. Putz [d], U. Müller [d]

[a] Nanocyl S.A. Rue de l'Essor-4, 5060 Sambreville, Belgium
[b] Departement of Metallurgy and Materials Engineering Katholieke Universiteit, Max–Planck Institute for Iron Research, Leuven Kasteelpark Arenberg 44, B-3001 Leuven, Belgium
[c] Max–Planck-Institute for Iron Research, Max–Planck-Street 1, 40237 Duesseldorf, Germany
[d] Kompetenzzentrum Holz GmbH, St. Peter Street 25, 4021 Linz, Austria

ARTICLE INFO

Article history:
Received 29 February 2008
Received in revised form 26 August 2008
Accepted 27 August 2008
Available online 13 September 2008

Keywords:
A. Wood
A. Polymer–matrix composites (PMCs)
B. Mechanical properties
C. Stress concentration
D. Non-destructive testing

ABSTRACT

The structural integrity of polypropylene (PP) matrix composites reinforced by natural wood fibers is investigated by digital image correlation (DIC) coupled with tensile tests. The use of the material as an alternative construction material requires extensive understanding of its micromechanical properties, which primarily define its performance. Addition of several additives such as coupling agents is common practice for such materials. These ingredients improve the performance of these materials mainly by improvement of the chemical and physical interactions between the nonpolar matrix and the polar wood fibers. These interactions facilitate the transfer of the applied deformation particularly in the interphase region between the polymer matrix and the reinforcing fibers. Such localized changes can influence the performance of the material specially its micromechanical behavior. The DIC via photogrammetry was used to study the spatial distribution of the accumulated plastic surface strain, which is based on pattern recognition of the surface before and after straining. The heterogeneous strain distribution reveals a structural inhomogeneity of the material. The magnitude of local strain was much higher than the global strain, suggesting preferred regions for plastic deformation formed by the microstructure.

1. Introduction

The macroscopic behavior of thermoplastic composites depends not only on the properties of their individual constituents but also on the elastic–plastic interaction between the different phases. When such complex composite materials are subjected to external mechanical loads, the lateral distribution of the accumulated residual deformation is heterogeneous entailing strain localization. This strain localization may lead to the crack initiation by micro-void formation and its coalescence in the matrix material or by debonding of the interfaces between the matrix and the fibers preceding the actual failure event.

The addition of fillers, such as natural fibers, influences density, stiffness and visco-elastic behavior of a polymer [1]. Good interfacial adhesion between the matrix and fibers is essential to transfer a stress from the matrix to the fibers and thus improve the mechanical strength of composites. The role of a coupling agent in wood fiber-reinforced plastic composites is very significant by improving compatibility and adhesion between polar wood fiber and nonpolar polymer matrices. By using coupling agents following mechanisms can be observed (1) formation of chemical bondings (ester bondings) between the fiber and the matrix, (2) reduction of the surface energy of the wood fiber which lowers the static interactions between the fibers (more homogeneous fiber distribution) as well as (3) improvement of the physical penetration of the plastic matrix into the microstructure of wood particles and fiber causing mechanical interlocking. Maleinated polypropylene (MAPP) is widely used as coupling agents in PP-natural fiber composites. The performance of MAPP as coupling agent for PP–wood-composites depends on the content of grafted maleic anhydride groups and on the polymer chain length. A higher content of grafted maleic anhydride groups improve the interaction between wood and the matrix, while high polymer chain length facilitate the co-crystallization of MAPP in the PP matrix [2]. Arbelaiz et al. [3] studied the influence of amount and type of copolymer (MAPP) as a compatibilizer on mechanical properties of flax fiber bundle/polypropylene composites. The use of MAPP as coupling agent improved mechanical properties and reduced the water uptake of composites by enhancing the adhesion between flax fiber bundles and PP. Beg and Pickering [4] investigated the

* Corresponding author. Address: Departement of Metallurgy and Materials Engineering Katholieke Universiteit, Max–Planck Institute for Iron Research, Leuven Kasteelpark Arenberg 44, B-3001 Leuven, Belgium. Tel.: +32 472339179.
E-mail addresses: agodara@nanocyl.be (A. Godara), d.raabe@mpie.de (D. Raabe), i.bergmann@kplus-wood.at (I. Bergmann), r.putz@kplus-wood.at (R. Putz), ulrich.mueller@kplus-wood.at (U. Müller).

0266-3538/$ - see front matter © 2008 Published by Elsevier Ltd.
doi:10.1016/j.compscitech.2008.08.031

combined effect of pretreatment of fiber with NaOH and coupling with MAPP on the physical and mechanical properties of radiata pine (*Pinus radiata*) fiber and PP matrix based composites. The authors showed, that without coupling agent, the tensile strength of the composites decreased with increasing fiber content, whereas with coupling agents, both tensile strength and Young's modulus increased with increasing fiber content. Scanning electron micrographs of the fractures surfaces suggested that the improvement in the interfacial bonding was most likely responsible for these improvements.

However, above a certain concentration of the coupling agent, deterioration of the mechanical properties often occurs [5–7]. It was found that in wood–polypropylene composites, in which MAPP with higher concentrations of grafted maleic anhydride is added, the functional groups are not only located at the interface to the wood fibers, but also tend to form a separated phase distributed within the PP matrix, affecting its properties [5,6]. The MAPP domains strongly affect the mechanical properties and deformation behavior of the composites. At high and constant concentration of the coupling agent, increasing the grafting level of maleic anhydride above a certain limit does not provide additional improvement of the tensile and impact strength of the wood filled composites. The dispersed MAPP particles act as stress concentrators similar to other modifier particles and after debonding at the interface initiate plastic deformation of the matrix by shear yielding. Bledzki et al. [7] performed similar investigations and reported the influence of MAPP on the mechanical properties of PP/hardwoodflour and soft-wood-flour composites and established that the composites displayed better properties at lower percentages of MAPP (5 wt.%). The authors arrived the general conclusion that in order to produce polymer composites with acceptable mechanical performance, a careful selection of coupling agents and optimization is needed [8].

Furthermore, PP with higher molecular weight revealed stronger interfacial interaction with cellulose in the composites [9] compared to a lower molecular weight PP and the composites derived from higher molecular weight of PP exhibited stronger tensile strength at the same cellulose content. Modification of wood fibers with anhydrides (acetic acid, maleic acid, succinic acid) also leaded to an improvement of the interfacial interactions between wood fibers and polypropylene matrices [10]. The addition of more than one compatibilizing agent is reported to induce stronger interfacial adhesion [11].

In general the mechanical properties of wood and PP are characterized by high differences. On the other hand the mechanical properties of wood are heavily influenced by the load direction meaning approx. 10-fold higher strength properties in axial direction than perpendicular to the grain. Beside the maximum strength also the stiffness of wood depends on the load direction. Therefore, the orientation of the wood particles and fibers in a certain composite also affect the mechanical properties.

The complex structure of solid wood and wood composites include irregularities, which can attract considerable stress concentrations. Sretenovic et al. [12] investigated the mechanism of stress transfer from the plastic matrix to the wood particles and vice versa. For this purpose tensile tests on a single-fiber wood plastic composite model were performed. The strain distribution around the particle was measured by means of electronic speckle pattern interferometry (ESPI). Additionally, an analytical analysis and finite element modelling of strain and stress distribution within the wood plastic composite was performed. The study proved that stresses are transferred not only along the fiber length corresponding to classical shear-lag model assumptions. Additionally, a significant proportion of axial stress is transferred across the interface between the fiber ends and the matrix, which is mainly achieved by good mechanical interlocking.

Owing to these experimental results [1–12], a better understanding of the microscopic behavior, in particular the distribution of the plastic micro-strains in these novel wood composites is needed. Strain-field analysis via digital image correlation also referred as photogrammetry is a powerful tool, that can be applied to map lateral strain distributions at different length scales. It allows a detailed investigation of complex micromechanical questions that are associated with the lateral distribution of the strain in heterogeneous materials [13–17]. The similar procedure is followed to resolve the influence of the amount of coupling agent, biopolymers and the inorganic fillers on the structural integrity of the wood reinforced PP composite material.

2. Experimental methods

2.1. Materials

The polymer matrix used was polypropylene homopolymer from Borealis (Type HD 120 MO) with a melt flow index of 8 g/10 min at 230 °C. The conifer wood fibers were selected with particle sizes between 150 and 500 μm with a moisture content of 5% (Type BK 40/90 from J. Rettenmaier & Söhne). The maleinated polypropylene (Orevac CA 100, Arcema) was used as a coupling agent. Acetylation of wood fibers was performed as described by Stallinger et al. [18]. Additionally the material was also modified by the various amounts of starch used as biopolymer and inorganic fillers.

2.2. Profile extrusion

The wood–PP composites (Table 1) containing 68–80% wood were produced by profile extrusion. Profile extrusion was performed in direct extrusion with a Cincinnati Fiberex T58 Extruder (conical twin screw extruder, screw design for wood polymer composites (WPC) extrusion, equipped with a Plasticolor dosing system and a Cincinnati TS Fiberex force feeding system. The tool for WPC extrusion (sheet die) and the down stream equipment was from Greiner Extrusionstechnik.

2.3. Tensile testing

The tensile tests were performed on a special miniaturized tensile test machine by Kammrath & Weiss GmbH (Germany). The computerized device features two moveable crossheads allowing the sample to remain in a stable centered position during testing, Fig. 2. The maximum capacity of the load cell amounts to 5000 N. The elongation speed amounted to 1 μm/s which translates to a strain rate of 10^{-3} s^{-1}. In order to record the deformation during the tensile tests, images were taken using two digital cameras adjusted perpendicular to each other whereby simultaneous imaging of both the top surface and the lateral surfaces of the sam-

Table 1
Composition of the extruded profiles

Material	Wood fibers (%)	Polypropylene (%)	Coupling agent (%)	Biopolymer (%)	Inorganic filler (%)
Wood75–PP25	75	25	0	0	0
Wood75acetylated–PP25	75	25	0	0	0
Wood75–PP22	75	22	3	0	0
Wood75–PP12	75	12	3	10	0
Wood80–PP17	80	17	3	0	0
Wood68–PP11	68	11	3	9	9

The various symbols such as Wood represents wood fibers, PP represents polypropylene, numerics after wood and PP represents the wt.% of wood fibers and PP, respectively, and acetylated represents acetylation of wood fibers.

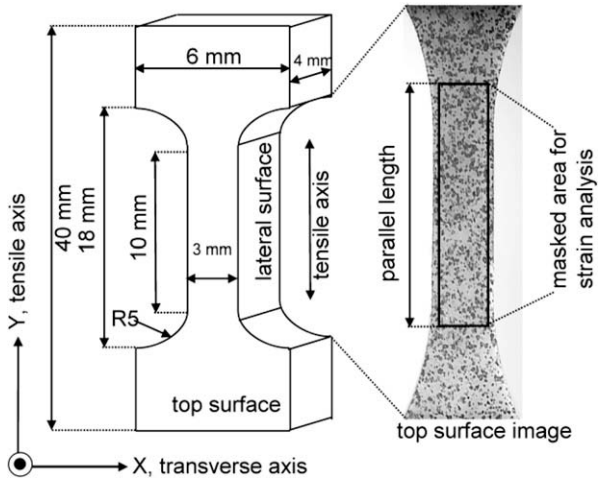

Fig. 1. The schematic illustration of the geometry of a tensile test specimen and the photograph of a spray-coated surface of a test specimen. The area of interest for the strain analysis is marked by a rectangle in the parallel length region.

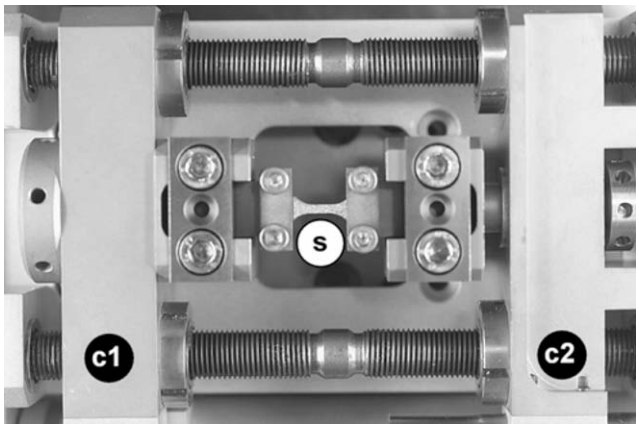

Fig. 2. Miniaturized tensile test rack with two moveable crossheads (c1, c2). The tensile specimen (s) which is mounted in the center has a length of 40 mm.

ple was possible. The cameras (CCD-1300: VDS Vosskühler GmbH, Weisse Breite 7, 49084 Osnabrück, Germany) which feature a resolution of up to 1300 dpi were equipped with lenses of 50 mm focal length and a maximum aperture of 2.8 (Schneider-Kreuznach, Ringstrasse 132, 55543 Bad Kreuznach, Germany). During testing the aperture was adjusted to the minimum value of 16 to achieve a maximal depth of focus. The camera set up is controlled by the ARAMIS system [19]. The cameras were mounted on a support positioning them perpendicular to the tensile test rack. The sets of digital gray scale pictures of the surface contrast were taken every 1 s which corresponds to an elongation of 10 μm which later served as input data for the digital image correlation method for calculating the displacement field.

2.4. Digital image correlation (DIC) via photogrammetry

DIC is a method that identifies 3D-coordinates of surface points and extracts displacement field and strain distribution by correlating subsequent sets of the image surface coordinates. The fundamental principle is based upon the fact that the distribution of grey scale values of a rectangular area (facet) in the undeformed state corresponds to the distribution of gray scale values of the same area in the deformed state as schematically shown in Fig. 3. The strain resolution is around 0.1%. The final strain map which was derived as the first order polar decomposition approximation of the displacement gradient tensor was then displayed in terms of the von Mises equivalent strain. The von Mises strain is given by the following equation

$$\varepsilon_M = \sqrt{[2/3(\varepsilon_{xx}^2 + \varepsilon_{yy}^2 + \varepsilon_{zz}^2) + 1/2(\gamma_{xy}^2 + \gamma_{yz}^2 + \gamma_{zx}^2)]} \quad (1)$$

where ϵ_{ii} indicates the normal strain components (Einstein summation rule does not apply) and γ_{ij} indicates shear strain components. Due to the two dimensional (surface) strain analysis conducted in this study, the strain tensor components ϵ_z, γ_{yz}, and γ_{zx} are unknown. This strain measure is a useful approximation of a deformation state which reduces a strain tensor to an equivalent scalar strain measure. Details of the method and determination of the characteristic data are described in [13–17,19,20].

Alternatively to the use of extensometers to calculate the global engineering strain (ϵ_g), global strain data can also be obtained by digital image correlation [19]. One simple and robust method consists in using the displacement field for evaluating the change in the spacing between two reference points upon loading. The initial length l_0 of the region of interest and the actual length l_i after each elongation interval give the global engineering strain ϵ_g according to $\epsilon_{g(i)} = (l_i - l_0)/l_0$, simply referred to as global strain in the following. The index i represents the deformation stage which is used as a reference state during the mechanical test. In case of a bone-like shaped flat standard tensile test specimen several such reference points can be defined at both ends of the parallel length of the specimen. These positions correspond to the points which serve in a standard test as contact coordinates for the edges of the extensometers. According to the formula above the average global strain can then be calculated for each deformation step.

For creating global mechanical tensile test curves the strain data are linked to the corresponding stress data. For the evaluation of Poisson's ratio additional reference points can be defined at both edges of the parallel length of the specimen. Similarly to the global strain, the strain in transverse direction ϵ_{tr} can be determined. Poisson's ratio is defined as the ratio of strain in transverse and in tensile direction in the linear elastic part of the stress strain curve according to $\nu = -\epsilon_{tr}/\epsilon_g$.

2.5. Sample preparation for surface mapping

The surface quality of the original image is the most crucial factor in determining the quality of the results obtained by the digital image correlation. Prior to the tensile tests the specimen surfaces were sprayed with a fine black colored acrylic resin based spray to create stochastic black and white contrast patterns for the subsequent DIC procedure. The test specimen was properly mounted and special precautions were taken to avoid any kind of illumination or shadowing effects.

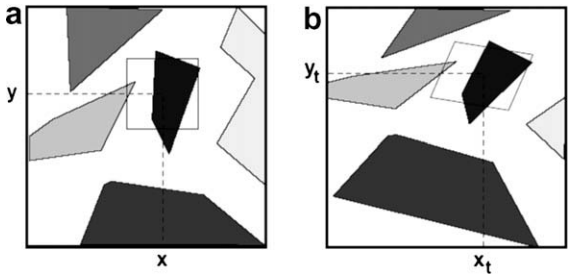

Fig. 3. Schematic drawing indicating (a) the initial pattern (before straining) and (b) the distorted pattern (after straining).

3. Results and discussion

3.1. Global tensile stress–strain behavior

The principal aspect of any composite material development is to optimize the quantity and the influences of various constituents added in order to improve the overall performance of the material. The performance can be influenced by both: by the major components and by the addition of smaller fraction constituents such as organic fillers and coupling agents. The main role of such small fraction constituents is to enhance the adhesion properties by modifying the interface between the different phases such as wood and polypropylene in the present study. The mechanical response of the different materials tested in this study reflects a noticeable influence of varying the amounts of different constituents (Fig. 4).

During processing of a polymer–matrix composite material, the interaction between the surfaces of the wood, the inorganic fillers or the biopolymer and the semi-crystalline polymer matrix such as PP may create various chemical and morphological inhomogeneities. These are typically discussed in terms of two distinct regions, namely, the interface and the interphase zones, respectively. The inter*face* is defined at the atomic scale as the layer of the immediate chemical bond between the fiber and the polymer matrix. The inter*phase* region is much larger. It is formed by local changes of the polymer matrix in the vicinity of a fiber. In these region local properties like morphology, thermo-mechanical behavior, and chemical composition can differ from the corresponding values observed in the bulk polymer matrix. This is explained by the cumulative influence of the enhanced rate of nucleation during the crystallization process and the parallel alignment of polymer chains along the solid surfaces provided by the different additives [21]. The author described the formation of such different regions in terms of transcrystallinity. Devaux and Chabert [22] showed the presence of a transcrystalline phase when organic fibers were added to polypropylene. They indicated that the transcrystallinity is directly linked to the topography of the organic fillers.

Such microstructural changes occurring due to addition of the various fillers, which altered the overall mechanical response, can also influence the distribution of the applied load, as presented in the strain mapping Section 3.2. The probable reasons for the different mechanical behavior produced due to the systematic variation of different constituents are discussed below.

3.1.1. Influence of wood acetylation (Wood75–PP25 and Wood75acetylated–PP25)

Acetylation of wood is performed to improve the structural integrity by stabilizing the cell wall, improving dimensional stability and environmental degradation [23–25]. The transformation of the hydroxylgroups of hemicellulose and lignin into acetylgroups lead to a lower polarity and so a higher compatibility between the wood fibers and the nonpolar PP matrix. Such effects enhance the efficiency of the interface/interphase in transferring the applied load between the wood and the PP in the present case [26]. Our results (Fig. 5) are consistent with these observations and showed that the acetylated wood–composite (Wood75acetylated–PP25) is higher in strength by almost 90% than the material prepared without the acetylation of wood (Wood75–PP25). The higher elastic modulus (~60%) and the decreased failure strain (~20%) of the composite with acetylated wood result from the increased interfacial properties.

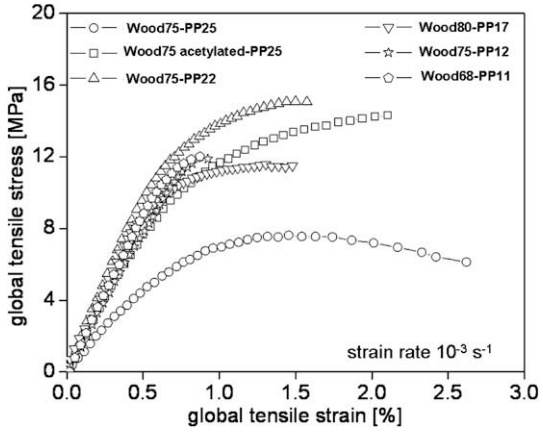

Fig. 4. Global tensile stress–strain behavior of the wood–polypropylene composites.

3.1.2. Influence of coupling agent (Wood75–PP25 and Wood75–PP22)

The mechanical response of adding the coupling agent clearly visible both in terms of the increased failure strength (Wood75–PP22, ~110%) and the decreased failure strain (~50%), Table 2. This indicates the higher effectiveness of adding the coupling agent in comparison with acetylation of wood. This is attributed to the different mechanisms of actions followed by the acetylation of wood and the addition of coupling agent. The acetylation process mainly improves the interfacial adhesion properties by modifying the surface properties of the wood, therefore its influence is more on the interface than on the interphase. The addition of coupling agent increases the compatibility between the hydrophilic wood material and hydrophobic matrices (binders) and entanglement between the PP and its molecules. This results in improved interphase properties and a lower strain to failure of the composite [27].

3.1.3. Influence of wood/polymer ratio (Wood75–PP22 and Wood80–PP17)

When the amount of polypropylene is decreased from 22 wt.% (Wood75–PP22) to 17 wt.% (Wood80–PP17), it reduces the failure strain by ~10% with corresponding decrease in the failure stress by ~20%. This is coherent with an observation that large amount of PP forms a better adhesive network across the wood phase. However, the elastic modulus is not significantly influenced.

3.1.4. Influence of a biopolymer at constant wood content (Wood75–PP22 and WPP7512)

An additional amount of the starch with decreased amount of PP (Wood75–PP12) seems to improve the interfacial properties, which is displayed by the increased failure strain ~20%. The decreased amount of PP from 22 wt.% to 12 wt.% is expected to alter the adhesive network but it seems that addition of the biopolymer, which is an organic filler, is contributing well in the formation of a good interpenetrating adhesive network. This is probably because the coupling agent does not only improve the interphase between wood and PP but also between the biopolymer and the PP.

3.1.5. Influence of inorganic fillers (Wood75–PP12 and Wood68–PP11)

Introducing an inorganic filler (Wood68–PP11) also modifies the mechanical behavior by making the material stiffer, which is characterized by the significantly decreased failure strain ~60%. The inorganic filler could also influence crystallization process by inducing heterogeneous nucleation thereby increasing overall crystallinity which could increase brittleness and the elastic modulus.

3.2. Qualitative analysis of the localized strain

Under applied external stress the solid materials elongate and get strained. The constitutive behavior, *i.e.*, the stress and strain relation generally is linear for small stresses. After reaching the elastic limit, the weakest parts of the sample tend to get destabi-

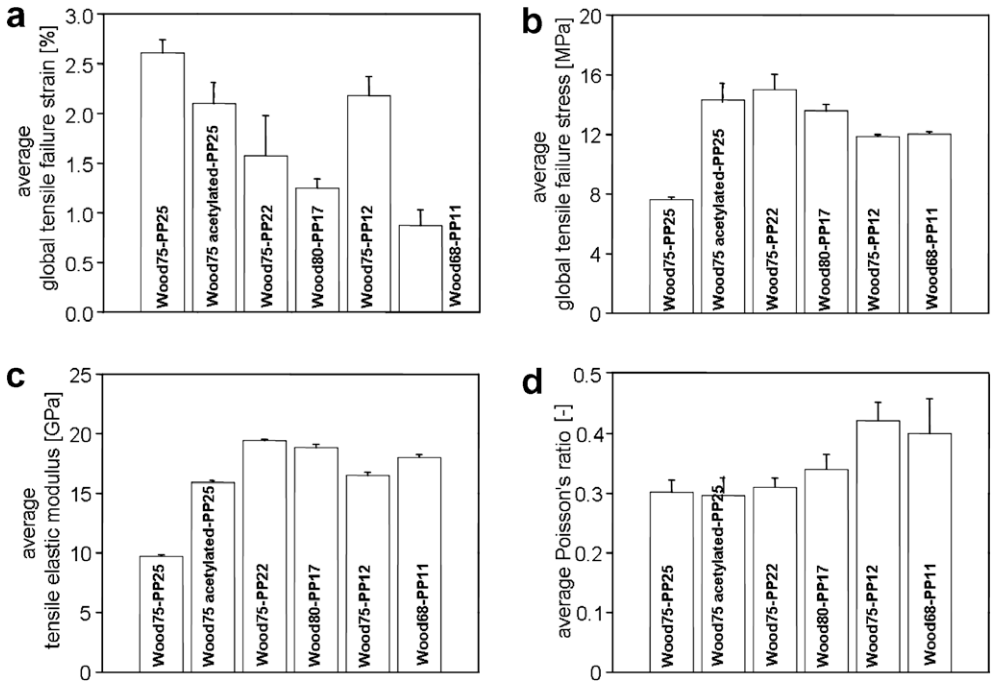

Fig. 5. Summarizes the characteristic mechanical data obtained from the set of five tensile tests performed for each specimen, namely the elastic modulus E, the failure strain ϵ_f, the failure stress σ_f and the Poission's ratio υ. These values are not absolute characteristic-values of the material but are derived to analyze the qualitative influence of the material composition on the overall performance of the material.

Table 2
Summary of the parameters used for DIC procedure

Measured field size on the specimen surface	3 × 10 mm (316 × 1050 pixels)
Project parameter: facet	
Facet size	15 pixels
Step size (distance between centers of two facets)	7 pixels
Project parameter: strain	
Computation size	3
Validity code	55%
Strain computation method	Total
Stage parameter	
Accuracy	0.04 pixels
Iteration limit	Enabled
Residual gray scale level	20 gray levels
Intersection deviation	0.3
Recording image sequence	
Simple measuring mode	1 image/s

lized and microscopic internal failures are noted. Those weakest parts often referred as nucleation centers, due to crack evolution around them, play a major role in the breakdown properties. In that way, the internal structure of the sample is damaged and the nonlinearity appears in the stress–strain behavior. Finally at a critical stress value, depending on the material, the amount of disorder and the specimen size, the macroscopic fracture occurs. Therefore, the evolution of such localized strain was investigated with the DIC and the influence of varying the amount of different constituent was observed. The strain distribution was calculated for the predefined area in the parallel length region of the test specimens Fig. 1. For each test specimen, four strain maps with increasing global engineering strain ϵ_g are displayed. The selected strain levels for Wood75–PP25, Wood75–PP22 and Wood75–PP12 are 0.3%, 0.5%, 1.0% and the strain value just before fracture. The failure strain for Wood80–PP17 and Wood68–PP11 was much smaller therefore the selected strain levels for these materials are 0.02%, 0.3%, 0.6% and the strain value just before fracture. The mapped local strain is displayed in terms of von Mises strain ϵ_M. The scale range was set constant equivalent to the highest localized value in the stage just before the fracture.

All the materials (Fig. 6) in general showed a heterogeneous strain pattern with relatively even distribution in the form of high strain domain (HSD) and low strain domain (LSD). The high strain domains are more pronounced at the edges which are probably due to the propagation of preexisting microcracks being easier at the free edges than in the middle of the sample. Such microcracks are probably caused by producing the bone-shaped samples. This effect promotes the damage accumulation away from the free edges and the coalescence of the generated micro-voids. The micro-voids could have formed due to non-uniform adhesion or to the delamination of the interface. Such localized failure of the microstructure results in the localized accumulation of strain, which is more pronounced at the edges and well captured by the DIC procedure. The random orientation of HSD and LSD and their overall pattern is preserved with increasing global strain while the level of local strain is elevated. The merging of higher strain domain occurs before fracture and leads to abrupt failure of the test specimen.

However, the comparison between the localized strain values clearly reflects the influences of the amount of PP and adding other constituents. For instance in Fig. 6a and b, Wood75–PP25 and Wood75acetylated–PP25, respectively, the materials shows highly localized HSD which is explained by the large plastic deformation of the region and supposedly due to the large amount of PP. As the PP contents are decreased (Fig. 6c–f), the numbers of HSD increased but with much lower levels of localized strain. The decreased amount of PP modifies the microstructure resulting in less number of such big pockets formed by large amount of PP or in other words increased global microstructural homogeneity. The higher strain localized region could also be formed by the localized failure mechanisms like debonding, microcracks, microvoids and their subsequent coalescence. These mesoscale deformation mechanisms are more pronounced as PP content is decreased to 11 wt.% (Fig. 6f – Wood68–PP11). The addition of coupling agent

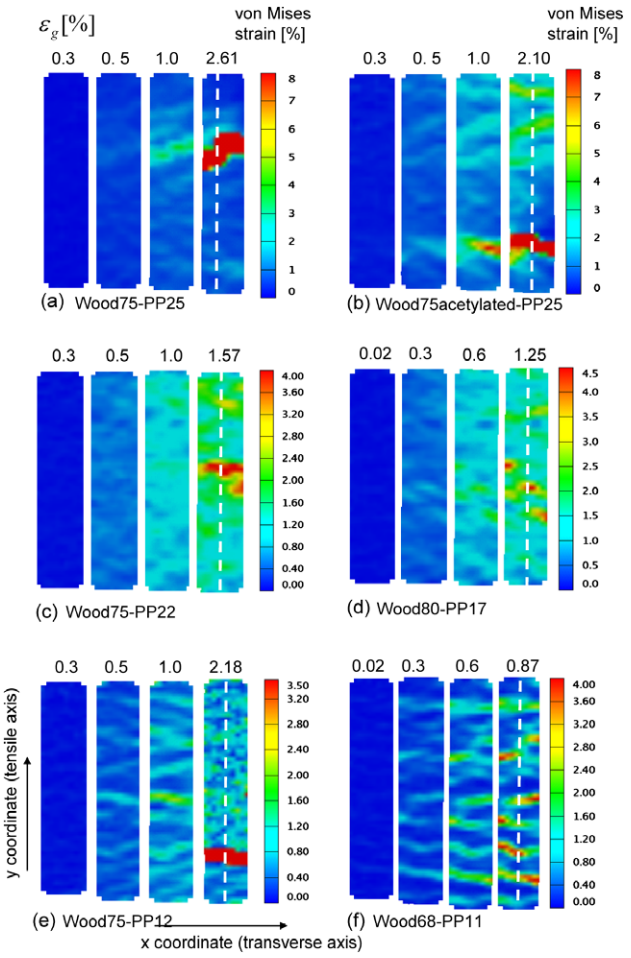

Fig. 6. The spatial distribution of the von Mises strain for the different wood–polypropylene composites: (a)–(f). The strain mapping was performed simultaneously the top surface. The global applied tensile strain (ϵ_g (%)) is shown on the top of each stage. The white dotted line in the strain maps marks the position of section for the strain profile.

and inorganic fillers compensated such changes which are clearly seen in overall increase in mechanical performance of the various materials (Fig. 5).

3.3. Quantitative analysis of the localized strain

In order to make quantitative analysis of the accumulated strains at the high strain domains (HSD) and at the low strain domains (LSD), sectional analysis was performed. The position of the section along the tensile axis was selected after observing the localized strain in the strain map just before fracture (marked with white dotted line, Fig. 6). The four curves in Fig. 7 display the evolution of the von Mises strain at each level of global applied strain ϵ_g (%) for each test specimen.

3.3.1. Sectional analysis of the localized strain

Fig. 7 shows the von Mises strain evolution profile at the top surface for the strain maps shown in Fig. 6. The accumulation of the strain is heterogeneous as indicated by the formation of periodic strain-maxima and strain-minima. The difference between the maxima and the minima is not very significant during the initial stages of deformation but it is pronounced as the applied global strain is increased. The materials with higher content of PP (Fig. 7a and b) show a single pronounced peak indicating highly localized strain region. This is possibly because of the plastic flow of the region formed by higher content of PP undergoing plastic deformation. Generally, if once such region starts flowing plastically, it acts as the point of maximum applied energy absorption or damage accumulation preventing other regions undergoing any significant damage. The acetylation of wood (Fig. 7b – Wood75acetylated–PP25) does not change this behavior at mesoscale because of the similar PP contents but improves global mechanical behavior like modulus and strength owing to the improved interface/interphase properties (Fig. 5a and b). As the PP content decreased, such highly localized strain accumulation behavior is transformed into several simultaneously growing peaks as seen in Fig. 7c–f. This suggests that the applied strain is distributed all over the sample due to increased stress transfer efficiency causing increased number of regions undergoing plastic deformation. In Fig. 7c there is small change in strain accumulation pattern shown by the two big peaks and the increased level of strain accumulation the smaller peaks is supported well by decreased PP content (22 wt.%). In Fig. 7d–f, the increased number of peaks and the lower levels of accumulation strains suggest a strong cumulative influence of ratio of wood fiber/PP contents, adding the biopolymer, and adding inorganic filler in modifying the internal microstructure of the materials especially the interface/interphase. For instance, in Fig. 7d, increased wood surface (80 wt.%) to reduced PP content (17 wt.%) should have made structure weak because of preassumed weaker adhesive network. But additional 3 wt.% of coupling agent compensated it by improving the interphase. This combination made microstructure stiffer (Fig. 5c) and improved strength (Fig. 5b) by inducing global microstructural homogeneity and caused several regions undergoing plastic deformation (increased number of peaks – Fig. 7d), which increased the probability of their coalescence thereby causing decrease in overall failure strain (Fig. 5a). Similar explanation could be given for the sample Wood68–PP11 represented in Fig. 7f which contains least amount of PP (11 wt.%) in combination with coupling agent (3 wt.%) and inorganic filler (9 wt.%). Fig. 7e represents the sample containing biopolymer which besides improving interfacial adhesion could also acts as plasticizing agent. This is seen by the increased number of peaks with a single higher strain accumulation peak representing a region undergoing maximum plastic deformation or damage accumulation. Such behavior prevented smaller peaks (regions) to grow and to follow the mechanism of coalescence and causing an abrupt failure. Instead, only one region deformed plastically increasing overall failure strain (Fig. 5a).

The systematic study carried out in the present work could be extended to other polymer composite systems. The local strain accumulation behavior reflects systematic progression of localized microstructural damage, which starts with strain localization at region such as large pocket of matrix, debonding, fiber breakages, pores, etc. This is followed by coalescence, i.e., damage accumulation and ultimately forming a major crack. The different constituents such as fibers, fillers, and the matrix itself influence the formation and growth mechanism of cracks. The quantitative analysis of the accumulated strain could reveal insights of the structural integrity of a microstructure like the level of accumulated strain and the number of peaks.

4. Conclusions

In this study, we investigated the structural integrity of wood–polypropylene composites in terms of change in physio-mechanical response by systematic variation of the different constituents such as wood, polypropylene, coupling agent, and biopolymer as filler. The overall stress–strain behavior of the materials and the distribution of the applied strain by microstrain mapping both reflected the effects of various constituents.

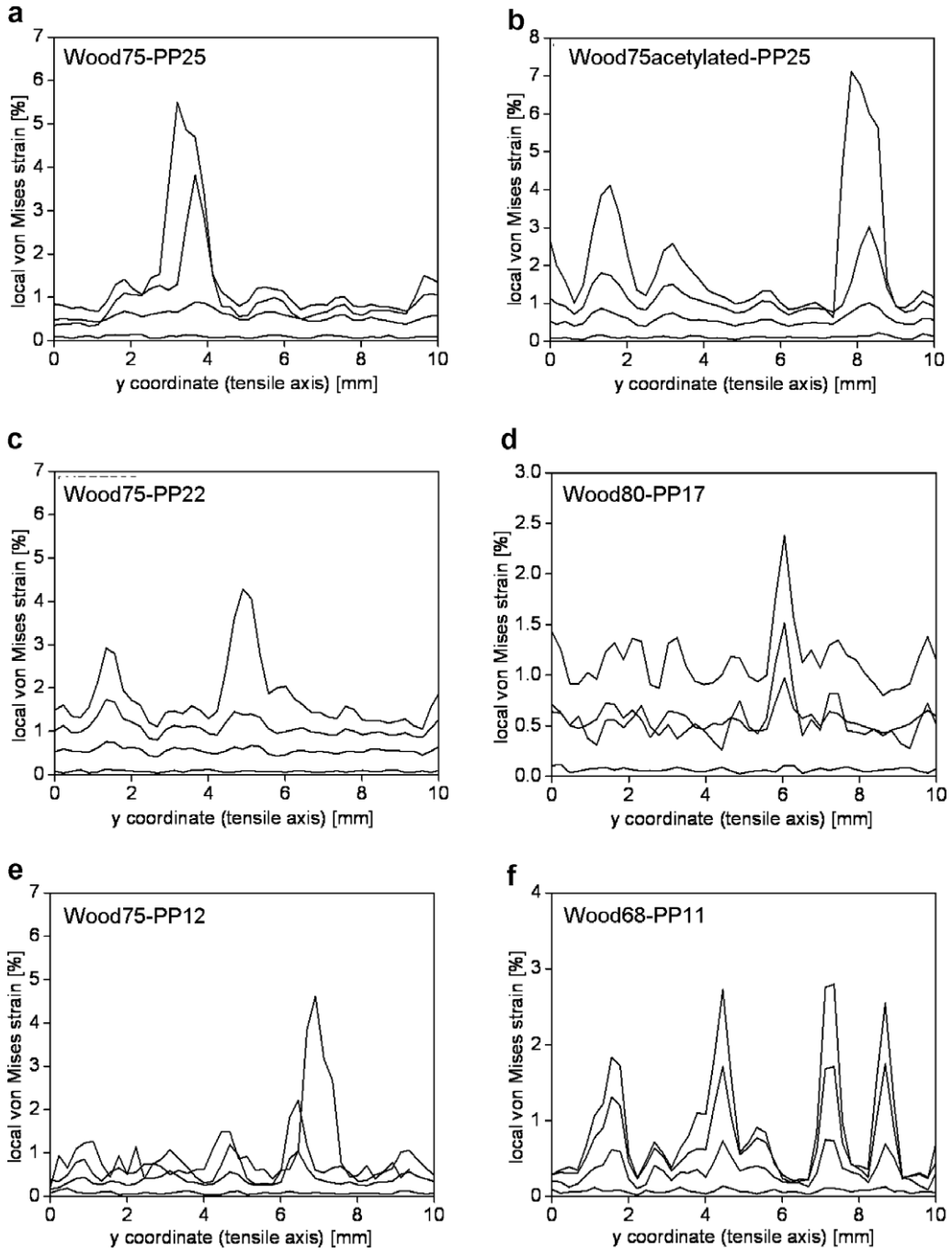

Fig. 7. Strain analysis for the wood/PP composite specimens along the positions marked by the white dotted line in the strain maps shown in Fig. 5. The evolution of the local von Mises strain for the test specimens: (a) Wood75–PP25; (b) Wood75acetylated–PP25; (c) Wood75–PP22; (d) Wood80–PP17; (e) Wood75–PP12; (f) Wood68–PP11.

The decreased amount of polypropylene significantly reduced ductility but in combination with other fillers substantially increased strength and elastic modulus of the material. The addition of coupling agent proved to be more efficient then acetylation in increasing overall mechanical performance (stiffness and strength) and inducing global microstructural homogeneity (distributed localized strain). The addition of biopolymer as organic filer showed plasticizing effect on interphase whereas addition of inorganic filler induce brittleness. At the mesoscale, the local strain patterns were found to be heterogeneous and corresponded well to the underlying modified microstructure of the material as a result of different matrix and filler contents. The quantitative analysis of localized accumulated strain revealed the critical details of the microstructural modifications, failure mechanisms and suggested that contents of different phases can alter the microstructure of a material significantly at mesoscale.

References

[1] Kausch HH, Beguelin Ph. Macromol Symp 2001;169:79.
[2] Kazayawoko M, Balatinecz JJ, Matuana LM. J Mater Sci 1999;34:6189.
[3] Arbelaiz A, Fernández B, Ramos JA, Rategi A, Llano-Ponte R, Mondragon I. Compos Sci Technol 2005;65:1582.
[4] Beg MDH, Pickering KL. Mater Manuf Process 2006;21:303.
[5] Hristov V, Krumova M, Michler G. Macromol Mater Eng 2006;291:677.
[6] Hristov VN, Krumova M, Vasileva S, Michler GH. J Appl Polym Sci 2004;92:1286.

[7] Bledzki K, Faruk O, Huque M. Polym Plast Technol Eng 2002;41:435.
[8] Karmaker AC, Schneider JP. J Mater Sci Lett 1996;15:201.
[9] Wulin Qiu, Takashi Endo, Takahiro H. Eur Polym J 2006;42:1059.
[10] Mahlberg R, Paajanen L, Nurmi A, Kivistö A, Rowell RM. Holz Roh Werkst 2001;59:319.
[11] Qiu W, Zhang F, Endo T, Hirotsu T. J Mater Sci 2005;40:3607.
[12] Sretenovic A, Müller U, Gindl W. Compos A Appl Sci Manuf 2006;37:1406.
[13] Zaefferer S, Kuo J-C, Zhao Z, Winning M, Raabe D. Adv Eng Mater 2003;51:563.
[14] Raabe D, Sachtleber M, Zhao Z, Roters F, Zaefferer S. Acta Mater 2001;49:3433.
[15] Sachtleber M, Zhao Z, Raabe D. Mater Sci Eng A 2002;336:81.
[16] Godara A, Raabe D. Compos Sci Technol 2007;67:2417.
[17] Parsons EM, Boyce MC, Parks DM, Weinberg M. Polymer 2005;46:2257.
[18] Stallinger S, Tanczos I, Schmidt H, Bucka H. Acetylierung von Holz mit Isopropenylacetate. GÖCH Tage, Linz, Austria 2002..
[19] Handbook for the Aramis system by GOM mbh, Gesellschaft für Optische Meßtechnik, Version September 2006. Germany: Braunschweig; 2006.
[20] Sachs C, Fabritius H, Raabe D. J Struct Biol 2006;155:409.
[21] Zafeiropoulos NE, Baillie CA, Matthews FL. Compos A Appl Sci 2001;32:525.
[22] Devaux E, Chabert B. Polym Compos 1991;31:391.
[23] Liu FP, Michael P, Wolcott I, Douglas J, Gardner J, Rials TG. Compos Interface 1994;2:419.
[24] Morozova A. Final workshop of COST action E22. Estoril; 2004.
[25] Mahlberg R, Paajanen L, Nurmi A, Kivistö A, Koskela K, Rowell RM. Holz Roh Werkst 2001;59:319.
[26] Kalantar J, Drzal LT. J Mater Sci 1990;25:4186.
[27] Rowell RM. Property enhancement of wood composites. In: Rowell RM, Vigo T, Kinzig B, editors. Composite applications—the role of matrix, fibre and interface. New York: VCH Publishers; 1992 [chapter 4].